Acta Cryst E CRYSTALLOGRAPHIC COMMUNICATIONS

ISSN 2056-9890

Synthesis, crystal structure and Hirshfeld surface analysis of dimethyl 3-(3-bromophenyl)-6-methyl-7-oxo-3,5,6,7-tetrahydropyrazolo[1,2-*a*]pyrazole-1,2-dicarboxylate

Rahhal El Ajlaoui,[a,b]* Yassine Hakmaoui,[a] El Mostapha Rakib,[a,c] El Mostafa Ketatni,[a] Mohamed Saadi[d] and Lahcen El Ammari[d]

[a]Laboratory of Molecular Chemistry, Materials and Catalysis, Faculty of Sciences and Technics, Sultan Moulay Slimane University, Béni-Mellal, BP 523, Morocco, [b]Département de Chimie, Faculté des Sciences Appliquées Ait Melloul, Université IBN ZOHR, N10. BP 6146 Cité Azrou, Ait Melloul, 86150 Agadir, Morocco, [c]Higher School of Technology, Sultan Moulay Slimane University, BP 336, Fkih Ben Salah, Morocco, and [d]Laboratoire de Chimie Appliquée des Matériaux, Centre des Sciences des Matériaux, Faculty of Science, Mohammed V University in Rabat, Avenue Ibn Batouta, BP 1014, Rabat, Morocco. *Correspondence e-mail: r_elajlaoui@yahoo.com

Received 21 December 2021
Accepted 27 December 2021

Edited by W. T. A. Harrison, University of Aberdeen, Scotland

Keywords: crystal structure; tetrahydropyrazolo[1,2-a]pyrazolone; pyrazole-1,2-dicarboxylate; Hirshfeld surface analysis; hydrogen bonds.

CCDC reference: 2131209

Supporting information: this article has supporting information at journals.iucr.org/e

The title compound, $C_{17}H_{17}BrN_2O_5$, resulted from the 1,3-dipolar cycloaddition reaction between dimethyl acetylenedicarboxylate and (3-bromobenzylidene)-4-methyl-5-oxopyrazolidin-2-ium-1-ide in $CHCl_3$. The dihedral angle between the pyrazole rings (all atoms) is 32.91 (10)°; the oxo-pyrazole ring displays an envelope conformation whereas the other pyrazole ring adopts a twisted conformation. The bromophenyl ring subtends a dihedral angle of 88.95 (9)° with the mean plane of its attached pyrazole ring. In the crystal, the molecules are linked by C—H···O hydrogen bonds and aromatic π–π interactions with an inter-centroid distance of 3.8369 (10) Å. The Hirshfeld surface analysis and fingerprint plots reveal that the molecular packing is governed by H···H (37.1%), O···H/H···O (31.3%), Br···H/H···Br (13.5%) and C···H/H···C (10.6%) contacts. The energy framework indicates that dispersion energy is the major contributor to the molecular packing.

1. Chemical context

Tetrahydropyrazolo[1,2-*a*] pyrazolones have been studied for about forty years as analogues of penicillin and cephalosporin antibiotics (Jungheim & Sigmund, 1987; Jungheim *et al.*, 1987; Ternansky *et al.*, 1993; Konaklieva & Plotkin, 2003; Hanessian *et al.*, 1997) and have been developed as herbicides and pesticides (Kosower *et al.*, 1995), as antitumor agents and as potent drugs for the treatment of cognitive dysfunctions such as Alzhheimer's disease. Among a variety of reported synthetic approaches to these compounds (Khidre *et al.*, 2013; Li & Zhao, 2014; Svete, 2006), 1,3-dipolar cycloaddition has been shown to be effective (Stanley & Sibi, 2008; Kissane & Maguire, 2010; Pellissier, 2012). Until now, several 1,3-dipoles, such as azomethine ylides (El Ajlaoui *et al.*, 2015), nitrones (Jen *et al.*, 2000; Kano *et al.*, 2005; Suga *et al.*, 2005) and carbonyl ylides (Suga *et al.*, 2007; Nambu *et al.*, 2009; Padwa 2011), have been studied. Among them, *N*,*N*′-cyclic azomethine imines (Stanovnik *et al.*, 1998; Qiu *et al.*, 2014; Nájera *et al.*, 2015; Xu & Doyle, 2014), have been increasingly employed in cycloadditions for the synthesis of pyrazolones and the related dinitrogen-fused heterocyclic derivatives with significant biological activities (Ternansky *et al.*, 1993; Boyd, 1993; Muehlebach, *et al.*, 2009).

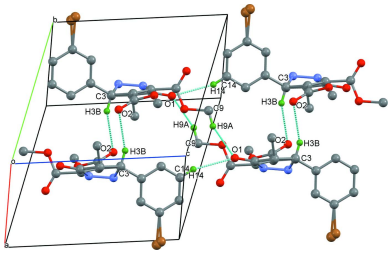

As part of our studies in this area, the title compound was synthesized and its molecular and crystal structure and Hirshfeld surface analysis are reported herein.

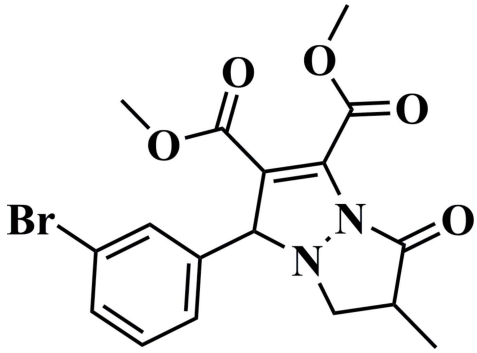

2. Structural commentary

The molecular structure of the the title compound is shown in Fig. 1. There are two stereogenic centres at C2 and C5: in the arbitrarily chosen asymmetric molecule, they have configurations of *S* and *R*, respectively, but a racemic mixture in the crystal is generated in the centrosymmetric $P\overline{1}$ space group. The structure is characterized by a disorder of the Br atom over two adjacent sites [Br···Br = 0.32 (2) Å]. The dihedral angle between the fused pyrazole rings (all atoms) is 32.91 (10)°. The C1–C3/N1/N2 oxo-pyrazole ring displays an envelope conformation on C3 whereas the C5–C7/N1/N2 pyrazole ring is twisted on N2—C5, as indicated by the following respective puckering parameters: $Q(2)$ = 0.2339 (19) Å, $\varphi(2)$ = 257.9 (4)° and $Q(2)$ = 0.2127 (16) Å, $\varphi(2)$ = 50.5 (4)°. Moreover, the mean plane passing through the oxo-pyrazole ring subtends a dihedral angle of 61.15 (10)° with the C12–C17 bromophenyl ring, which is practically perpendicular to the other pyrazole ring as indicated by the dihedral angle of 88.95 (9)°. The non-H atoms of the ester groups are virtually coplanar, the maximum deviations from the mean planes being 0.017 (2) Å at C10 for the O2/O3/C10/C11 grouping and 0.013 (1) Å at O5 for the O4/O5/C8/C9 grouping. The dihedral angle between these two planes is 62.15 (12)°.

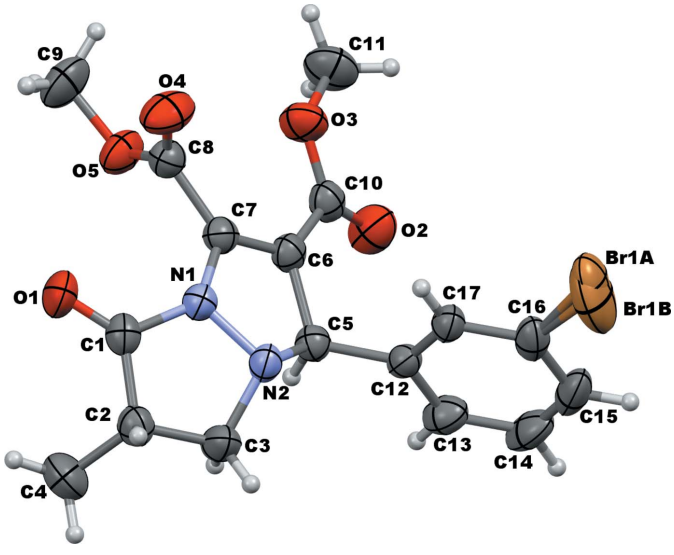

Figure 1
The molecular structure of the title compound showing displacement ellipsoids drawn at the 50% probability level.

Table 1
Hydrogen-bond geometry (Å, °).

D—H···*A*	*D*—H	H···*A*	*D*···*A*	*D*—H···*A*
C9—H9*A*···O1^{i}	0.96	2.42	3.258 (3)	146
C14—H14···O1^{ii}	0.93	2.53	3.418 (2)	161
C11—H11*B*···O2^{iii}	0.96	2.60	3.533 (3)	164
C3—H3*B*···O2^{iv}	0.97	2.62	3.514 (3)	154

Symmetry codes: (i) $-x+1, -y+1, -z+2$; (ii) $x, y, z-1$; (iii) $-x, -y+1, -z+1$; (iv) $-x+1, -y+1, -z+1$.

3. Supramolecular features

In the crystal, the molecules are linked by C—H···O hydrogen bonds: O1 accepts two such bonds and O2 and O3 accept one each (Table 1 and Fig. 2). The bromophenyl rings of adjacent molecules are linked by an aromatic stacking π–π interaction with an inter-centroid distance of 3.8369 (10) Å.

4. Database survey

A search of the Cambridge Structural Database (CSD, version 5.42, update of May 2021; Groom *et al.*, 2016) for the pyrazole-1,2-dicarboxylate unit revealed only one hit, namely refcode RICFUF: dimethyl 3-(*tert*-butylamino)-7-phenyl-5-oxo-1*H*,5*H*-pyrazolo[1,2-*a*]pyrazole-1,2-dicarboxylate (Abbasi *et al.*, 2007). The conformations of the fused pyrazole rings present in this compound and those of the title compound are different. Furthermore, the values of the dihedral angles between the planes passing through the rings are also very different, except for the angles between the fused pyrazole

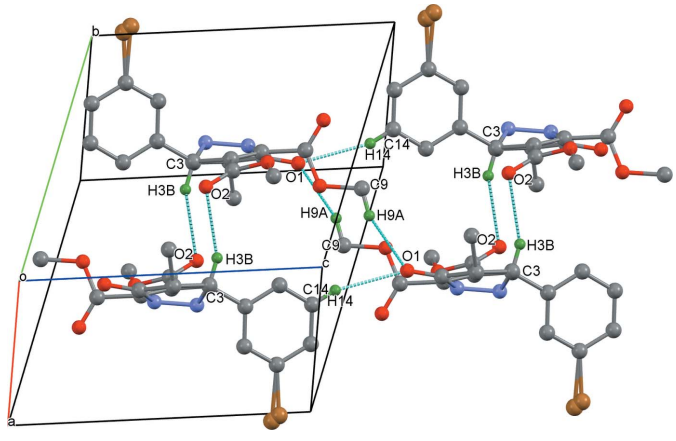

Figure 2
Crystal packing for the title compound showing hydrogen bonds as dashed blue lines.

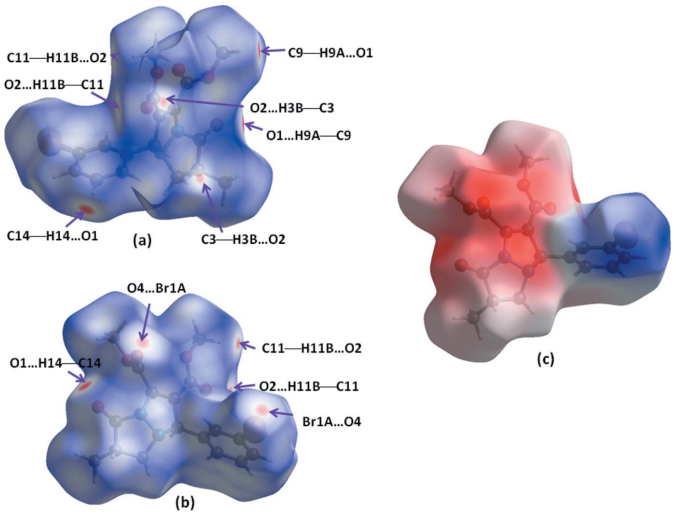

Figure 3
Hirshfeld surfaces of the title compound mapped over (*a*) and (*b*) d_{norm} to visualize the intermolecular C—H···O and Br···O contacts and (*c*) electrostatic potential energy using the STO-3 G basis set at the Hartree–Fock level.

rings, the difference of which does not exceed one degree, *i.e.* 34.13° in RICFUF and 32.91 (10)° in the title compound. It may be noted that the phenyl substituent is linked to the oxo-pyrazole ring and the two carboxylate groups to the other pyrazole ring in RICFUF, while in the title compound the phenyl and both carboxylate groups are linked to the same pyrazole ring.

5. Computational chemistry

Hirshfeld surface analysis

The Hirshfeld surface (HS) analyses (Spackman & Jayatilaka, 2009) and two-dimensional fingerprint plots (McKinnon *et al.*, 2007) generated using *CrystalExplorer17.5* (Turner *et al.*, 2017) show the various intermolecular interactions in the crystal structure. The three-dimensional d_{norm} surface of the title compound using a standard surface resolution with a fixed colour scale of −0.21 to 1.38 a.u is shown in Fig. 3*a*,*b*. The intense red spots on the surface are due to the C—H···O hydrogen bonds and C—H···Br contacts. The bright-red spots in Fig. 3*c* indicate atoms with the potential to be hydrogen-bond acceptors (negative electrostatic potential), while blue regions indicate atoms with positive electrostatic potential (hydrogen-bond donors) (Spackman *et al.*, 2008).

Two-dimensional fingerprint plots for the H···H, H···O/O···H, H···Br/Br···H and H···C/C···H contacts are presented in Fig. 4. The most important interaction is H···H ($d_e = d_i = 1.15$ Å) (Fig. 4*b*), contributing 37.6% to the overall crystal packing, which is reflected as widely scattered points of high density due to the large hydrogen content of the molecule. The contribution from the O···H/H···O contacts (31.4%), corresponding to C—H···O interactions, is represented by a pair of sharp spikes characteristic of a strong hydrogen-bond interaction ($d_i + d_e = 2.40$ Å, Fig. 4*c*). The reciprocal H···Br/Br···H interactions (12.8%) are present as two symmetrical broad wings with $d_i + d_e = 3.10$ Å (Fig. 4*d*). The C···H/H···C contacts contribute 10.8% to the Hirshfeld surface, featuring a wide region with $d_i + d_e = 2.95$ Å (Fig. 4*e*). The smaller percentage contributions of other types of contact are listed in Table 2.

Table 2
Percentage contributions of interatomic contacts to the Hirshfeld surface of the title compound.

Contact	Percentage contribution
H···H	37.1
O···H/H···O	31.3
Br···H/H···Br	13.5
C···H/H···C	10.6
N···H/H···N	2.1
O···Br/Br···O	1.9
C···C	1.9
C···N/N···C	0.7
O···N/N···O	0.3
Br···Br	0.3
N···N	0.2

Interaction energy calculations

The intermolecular interaction energies between molecules in the title compound computed using a B3LYP/6–31G (d, p)

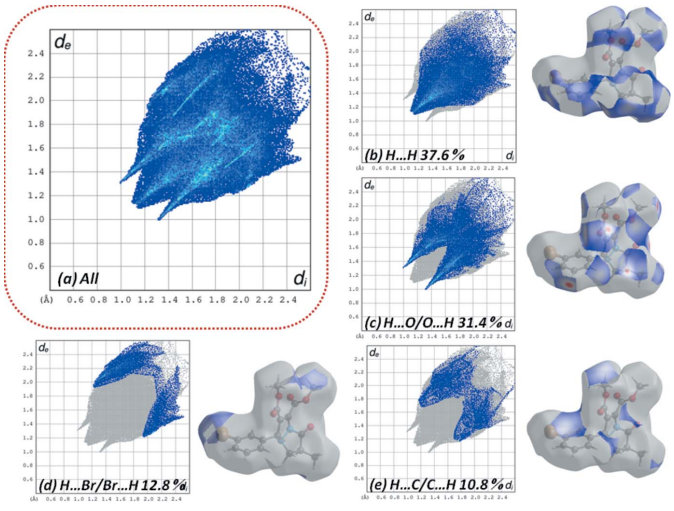

Figure 4
Two-dimensional fingerprint plots for the title compound showing (*a*) all interactions, and delineated into (*b*) H···H, (*c*) H···O/O···H, (*d*) H···Br/Br···H and (*e*) H···C/C···H interactions.

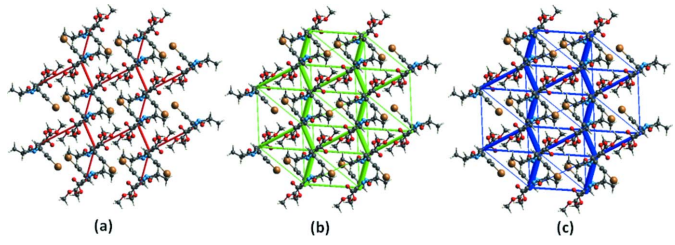

Figure 5
Energy framework of the title compound viewed along [001] showing (*a*) Coulombic energy, (*b*) dispersion energy and (*c*) total energy.

Table 3
Summary of interaction energies (kJ mol^{-1}) calculated for the title compound.

Contact	R (Å)	E_{ele}	E_{pot}	E_{dis}	E_{rep}	E_{tot}	Symmetry code
C11—H11*B*···O2	7.99	−15.9	−3.6	−36.5	26.5	−34.9	-*x*, −*y*, −*z*
C3—H3*B*···O2	6.38	−21.9	−6.9	−54.4	38.0	−52.1	-*x*, −*y*, −*z*
C14—H14···O1	11.09	−9.3	−2.6	−11.7	9.8	−15.9	*x*, *y*, *z*
C9—H9*A*···O1	11.96	−17.2	−4.4	−16.6	21.4	−22.6	-*x*, −*y*, −*z*
Br1*A*···O4	10.81	−14.3	−4.0	−22.4	15.9	−27.7	-*x*, −*y*, −*z*

energy model available in *Crystal Explorer 17.5* (Turner *et al.*, 2017), where a cluster of molecules was generated within a radius of 3.8 Å by default. The total intermolecular energy (E_{tot}) is the sum of electrostatic (E_{ele}), polarization (E_{pol}), dispersion (E_{dis}), and exchange-repulsion (E_{rep}) energies. The energy frameworks, which provide a view of the supramolecular architecture of crystals, are represented by cylinders joining the centroids of molecular pairs using red, green and, blue colour codes for the E_{ele}, E_{dis}, and E_{tot} energy components, respectively, with a cut-off value of 5 kJ mol^{-1} and a scale factor of 80 to all energy components (Fig. 5). The benchmarked energies E_{ele}, E_{pol}, E_{dis} and E_{rep} were scaled as 1.057, 0.740, 0.871 and 0.618, respectively (Mackenzie *et al.*, 2017). The nature and strength of the energies for the key identified intermolecular interactions are summarized in Table 3. The computed interaction energies for electrostatic, polarization, dispersion and exchange repulsion are −107.7 kJ mol^{-1}, −33.9 kJ mol^{-1}, −299.7 kJ mol^{-1} and 185.2 kJ mol^{-1}, respectively. These data reveal that the dispersive component makes the major contribution to the intermolecular interactions in the crystal. The calculations showed that the C3—H3*B*···O2 hydrogen bond has the greatest energy among all close contacts present in the crystal with its energy (–52.1 kJ mol^{-1}) having a major electrostatic contribution (–21.9 kJ mol^{-1}). The next most significant contribution, with a total energy of −34.9 kJ mol^{-1}, arises from the C11—H11*B*···O2 hydrogen bond. Lower energies, compared to the above interactions, are calculated for the Br1*A*···O4, C9—H9*A*···O1 and C14—H14···O1 contacts.

Frontier molecular orbital (FMO) calculations

The optimized structure of the title compound was established in the gas phase using density functional theory (DFT) using the B3LYP exchange correlation functional and basis-set calculations (Becke, 1993) as implanted in *GAUSSIAN 09* (Frisch *et al.*, 2009). The differences between calculated and experimental bond lengths and angles are within a few Ångstroms and degrees, respectively, when compared to the experimental parameters, which indicate that our calculations are acceptable (see supplementary Tables 1 and 2). The HOMO–LUMO gap of the molecule is calculated to be about 4.16 eV.

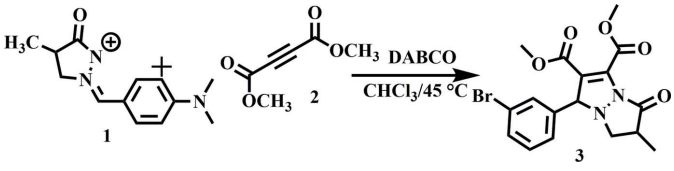

Figure 6
Scheme showing the synthesis of the title compound.

6. Synthesis and crystallization

To a solution of DMAD (dimethyl acetylenedicarboxylate; 0.2 mmol, 2 equiv.) in 10 ml of $CHCl_3$ containing a catalytic amount of DABCO (0.02 mmol, 0.2 equiv.), (3-bromobenzylidene)-4-methyl-5-oxopyrazolidin-2-ium-1-ide (0.10 mmol, 1 equiv.) was added (Fig. 6). The mixture was stirred at 318 K until the consumption of the azomethine imine was complete (monitored by TLC with 3:7 hexane/ethyl acetate *v*:*v*). After completion of the reaction, the residue was concentrated *in vacuo*. The crude product was purified by column chromatography on silica gel using hexane:ethyl acetate (2/8 *v*:*v*) as eluent. The title compound was recrystallized from ethanol solution in the form of colourless blocks (yield 68%, m.p. 383 K).

Table 4
Experimental details.

Crystal data	
Chemical formula	$C_{17}H_{17}BrN_2O_5$
M_r	409.23
Crystal system, space group	Triclinic, $P\overline{1}$
Temperature (K)	296
a, *b*, *c* (Å)	8.8579 (5), 10.5336 (6), 11.0893 (6)
α, β, γ (°)	62.282 (2), 75.437 (2), 88.241 (2)
V (Å^3)	882.03 (9)
Z	2
Radiation type	Mo *Kα*
μ (mm^{-1})	2.36
Crystal size (mm)	0.32 × 0.28 × 0.19
Data collection	
Diffractometer	Bruker D8 VENTURE Super DUO
Absorption correction	Multi-scan (*SADABS*; Krause *et al.*, 2015)
T_{min}, T_{max}	0.617, 0.746
No. of measured, independent and observed [$I > 2\sigma(I)$] reflections	27467, 3884, 3257
R_{int}	0.027
$(\sin\theta/\lambda)_{max}$ (Å^{-1})	0.641
Refinement	
$R[F^2 > 2\sigma(F^2)]$, $wR(F^2)$, *S*	0.027, 0.078, 1.04
No. of reflections	3882
No. of parameters	235
H-atom treatment	H-atom parameters constrained
$\Delta\rho_{max}$, $\Delta\rho_{min}$ (e Å^{-3})	0.23, −0.26

Computer programs: *APEX3* and *SAINT* (Bruker, 2016), *SHELXT2014/5* (Sheldrick, 2015*a*), *SHELXL2018/3* (Sheldrick, 2015*b*), *WinGX* and *ORTEP-3 for Windows* (Farrugia, 2012), *Mercury* (Macrae *et al.*, 2020) and *publCIF* (Westrip, 2010).

7. Refinement

Crystal data, data collection and structure refinement details are summarized in Table 4. Four reflections affected by the beamstop were omitted from the refinement. All H atoms were placed geometrically (C—H = 0.93–0.98 Å) and refined as riding atoms with U_{iso}(H) = 1.2U_{eq}(C) or 1.5U_{eq}(methyl C). The Br atom was modelled as disordered over adjacent sites in a 0.5862:0.4138 ratio.

Acknowledgements

The authors thank the Faculty of Science, Mohammed V University in Rabat, Morocco, for the X-ray measurements.

References

Abbasi, A., Adib, M. & Eriksson, L. (2007). *Acta Cryst.* E**63**, o2115–o2116.
Becke, A. D. (1993). *J. Chem. Phys.* **98**, 5648–5652.
Boyd, D. B. (1993). *J. Med. Chem.* **36**, 1443–1449.
Bruker (2016). *APEX3*, *SAINT* and *SADABS*. Bruker AXS Inc., Madison, Wisconsin, USA.
El Ajlaoui, R., Ouafa, A., Mojahidi, S., El Ammari, L., Saadi, M. & El Mostapha, R. (2015). *Synth. Commun.* **45**, 2035–2042.
Farrugia, L. J. (2012). *J. Appl. Cryst.* **45**, 849–854.
Frisch, M. J., Trucks, G. W., Schlegel, H. B., Scuseria, G. E., Robb, M. A., Cheeseman, J. R., Scalmani, G., Barone, V., Mennucci, B., Petersson, G. A., Nakatsuji, H., Caricato, M., Li, X., Hratchian, H. P., Izmaylov, A. F., Bloino, J., Zheng, G., Sonnenberg, J. L., Hada, M., Ehara, M., Toyota, K., Fukuda, R., Hasegawa, J., Ishida, M., Nakajima, T., Honda, Y., Kitao, O., Nakai, H., Vreven, T., Montgomery, J. A., Jr., Peralta, J. E., Ogliaro, F., Bearpark, M., Heyd, J. J., Brothers, E., Kudin, K. N., Staroverov, V. N., Kobayashi, R., Normand, J., Raghavachari, K., Rendell, A., Burant, J. C., Iyengar, S. S., Tomasi, J., Cossi, M., Rega, N., Millam, J. M., Klene, M., Knox, J. E., Cross, J. B., Bakken, V., Adamo, C., Jaramillo, J., Gomperts, R., Stratmann, R. E., Yazyev, O., Austin, A. J., Cammi, R., Pomelli, C., Ochterski, J. W., Martin, R. L., Morokuma, K., Zakrzewski, V. G., Voth, G. A., Salvador, P., Dannenberg, J. J., Dapprich, S., Daniels, A. D., Farkas, Ö., Foresman, J. B., Ortiz, J. V., Cioslowski, J. & Fox, D. J. (2009). *GAUSSIAN09*. Gaussian Inc., Wallingford, CT, USA.
Groom, C. R., Bruno, I. J., Lightfoot, M. P. & Ward, S. C. (2016). *Acta Cryst.* B**72**, 171–179.
Hanessian, S., McNaughton-Smith, G., Lombart, H. G. & Lubell, W. D. (1997). *Tetrahedron*, **53**, 12789–12854.
Jen, W. S., Wiener, J. J. M. & MacMillan, D. W. C. (2000). *J. Am. Chem. Soc.* **122**, 9874–9875.
Jungheim, L. N. & Sigmund, S. K. (1987). *J. Org. Chem.* **52**, 4007–4013.
Jungheim, L. N., Sigmund, S. K. & Fisher, J. W. (1987). *Tetrahedron Lett.* **28**, 285–288.
Kano, T., Hashimoto, T. & Maruoka, K. (2005). *J. Am. Chem. Soc.* **127**, 11926–11927.
Khidre, R., Mohamed, H. A. & Abdel-Wahab, B. F. (2013). *Turk. J. Chem.* **37**, 1–35.
Kissane, M. & Maguire, A. R. (2010). *Chem. Soc. Rev.* **39**, 845–883.
Konaklieva, M. I. & Plotkin, B. J. (2003). *Current Medicinal Chemistry - Anti-Infective Agents* **2**; 287–302.
Kosower, E. M., Radkowsky, A. E., Fairlamb, A. H., Croft, S. L. & Neal, R. (1995). *Eur. J. Med. Chem.* **30**, 659–671.
Krause, L., Herbst-Irmer, R., Sheldrick, G. M. & Stalke, D. (2015). *J. Appl. Cryst.* **48**, 3–10.
Li, M. & Zhao, B. X. (2014). *Eur. J. Med. Chem.* **85**, 311–340.
Mackenzie, C. F., Spackman, P. R., Jayatilaka, D. & Spackman, M. A. (2017). *IUCrJ*, **4**, 575–587.
Macrae, C. F., Sovago, I., Cottrell, S. J., Galek, P. T. A., McCabe, P., Pidcock, E., Platings, M., Shields, G. P., Stevens, J. S., Towler, M. & Wood, P. A. (2020). *J. Appl. Cryst.* **53**, 226–235.
McKinnon, J. J., Jayatilaka, D. & Spackman, M. A. (2007). *Chem. Commun.* pp. 3814.
Muehlebach, M., Boeger, M., Cederbaum, F., Cornes, D., Friedmann, A. A., Glock, J., Niderman, T., Stoller, A. & Wagner, T. (2009). *Bioorg. Med. Chem.* **17**, 4241–4256.
Nájera, C., Sansano, J. M. & Yus, M. (2015). *Org. Biomol. Chem.* **13**, 8596–8636.
Nambu, H., Hikime, M., Krishnamurthi, J., Kamiya, M., Shimada, N. & Hashimoto, S. (2009). *Tetrahedron Lett.* **50**, 3675–3678.
Padwa, A. (2011). *Tetrahedron*, **67**, 8057–8072.
Pellissier, H. (2012). *Tetrahedron*, **68**, 2197–2232.
Qiu, G., Kuang, Y. & Wu, J. (2014). *Adv. Synth. Catal.* **356**, 3483–3504.
Sheldrick, G. M. (2015*a*). *Acta Cryst.* A**71**, 3–8.
Sheldrick, G. M. (2015*b*). *Acta Cryst.* C**71**, 3–8.
Spackman, M. A. & Jayatilaka, D. (2009). *CrystEngComm*, **11**, 19–32.
Spackman, M. A., McKinnon, J. J. & Jayatilaka, D. (2008). *CrystEngComm*, **10**, 377–388.
Stanley, L. M. & Sibi, M. P. (2008). *Chem. Rev.* **108**, 2887–2902.
Stanovnik, B., Jelen, B., Turk, C., Žličar, M. & Svete, J. (1998). *J. Heterocycl. Chem.* **35**, 1187–1204.
Suga, H., Ishimoto, D., Higuchi, S., Ohtsuka, M., Arikawa, T., Tsuchida, T., Kakehi, A. & Baba, T. (2007). *Org. Lett.* **9**, 4359–4362.
Suga, H., Nakajima, T., Itoh, K. & Kakehi, A. (2005). *Org. Lett.* **7**, 1431–1434.
Svete, J. (2006). *Arkivoc*,**VII**, 35–56.
Ternansky, R. J., Draheim, S. E., Pike, A. J., Counter, F. T., Eudaly, J. A. & Kasher, J. S. (1993). *J. Med. Chem.* **36**, 3224–3229.
Turner, M. J., MacKinnon, J. J., Wolff, S. K., Grimwood, D. J., Spackman, P. R., Jayatilaka, D. & Spackman, M. A. (2017). *Crystal Explorer17.5*. University of Western Australia, Perth, Australia.
Westrip, S. P. (2010). *J. Appl. Cryst.* **43**, 920–925.
Xu, X. & Doyle, M. P. (2014). *Acc. Chem. Res.* **47**, 1396–1405.

supporting information

Acta Cryst. (2022). E**78**, 125-129 [https://doi.org/10.1107/S2056989021013621]

Synthesis, crystal structure and Hirshfeld surface analysis of dimethyl 3-(3-bromophenyl)-6-methyl-7-oxo-3,5,6,7-tetrahydropyrazolo[1,2-*a*]pyrazole-1,2-dicarboxylate

Rahhal El Ajlaoui, Yassine Hakmaoui, El Mostapha Rakib, El Mostafa Ketatni, Mohamed Saadi and Lahcen El Ammari

Computing details

Data collection: *APEX3* (Bruker, 2016); cell refinement: *SAINT* (Bruker, 2016); data reduction: *SAINT* (Bruker, 2016); program(s) used to solve structure: *SHELXT2014/5* (Sheldrick, 2015*a*); program(s) used to refine structure: *SHELXL2018/3* (Sheldrick, 2015*b*); molecular graphics: *WinGX* and *ORTEP-3 for Windows* (Farrugia, 2012); software used to prepare material for publication: *Mercury* (Macrae *et al.*, 2020) and *publCIF* (Westrip, 2010).

Dimethyl 3-(3-bromophenyl)-6-methyl-7-oxo-3,5,6,7-tetrahydropyrazolo[1,2-*a*]pyrazole-1,2-dicarboxylate

Crystal data

$C_{17}H_{17}BrN_2O_5$
M_r = 409.23
Triclinic, $P\overline{1}$
a = 8.8579 (5) Å
b = 10.5336 (6) Å
c = 11.0893 (6) Å
α = 62.282 (2)°
β = 75.437 (2)°
γ = 88.241 (2)°
V = 882.03 (9) Å^3
Z = 2
$F(000)$ = 416
D_x = 1.541 Mg m^{-3}
Mo $K\alpha$ radiation, λ = 0.71073 Å
Cell parameters from 3884 reflections
θ = 2.2–27.1°
μ = 2.36 mm^{-1}
T = 296 K
Block, colourless
0.32 × 0.28 × 0.19 mm

Data collection

Bruker D8 VENTURE Super DUO diffractometer
Radiation source: INCOATEC IμS micro-focus source
HELIOS mirror optics monochromator
Detector resolution: 10.4167 pixels mm^{-1}
φ and ω scans
Absorption correction: multi-scan (SADABS; Krause *et al.*, 2015)
T_{min} = 0.617, T_{max} = 0.746
27467 measured reflections
3884 independent reflections
3257 reflections with $I > 2\sigma(I)$
R_{int} = 0.027
θ_{max} = 27.1°, θ_{min} = 2.2°
h = −11→11
k = −13→13
l = −14→14

Refinement

Refinement on F^2
Least-squares matrix: full
$R[F^2 > 2\sigma(F^2)]$ = 0.027
$wR(F^2)$ = 0.078
S = 1.04
3882 reflections
235 parameters
0 restraints

Primary atom site location: structure-invariant direct methods
Secondary atom site location: difference Fourier map
Hydrogen site location: inferred from neighbouring sites

H-atom parameters constrained
$w = 1/[\sigma^2(F_o^2) + (0.0411P)^2 + 0.1854P]$ where $P = (F_o^2 + 2F_c^2)/3$
$(\Delta/\sigma)_{max} < 0.001$
$\Delta\rho_{max} = 0.23$ e Å^{-3}
$\Delta\rho_{min} = -0.26$ e Å^{-3}

Special details

Geometry. All esds (except the esd in the dihedral angle between two l.s. planes) are estimated using the full covariance matrix. The cell esds are taken into account individually in the estimation of esds in distances, angles and torsion angles; correlations between esds in cell parameters are only used when they are defined by crystal symmetry. An approximate (isotropic) treatment of cell esds is used for estimating esds involving l.s. planes.

Fractional atomic coordinates and isotropic or equivalent isotropic displacement parameters (Å^2)

	x	*y*	*z*	U_{iso}*/U_{eq}	Occ. (<1)
C1	0.59723 (18)	0.82071 (16)	0.63241 (16)	0.0400 (3)	
C2	0.73763 (18)	0.89402 (17)	0.50667 (16)	0.0426 (3)	
H2	0.747329	0.997326	0.477490	0.051*	
C3	0.69585 (19)	0.8717 (2)	0.39196 (17)	0.0543 (4)	
H3A	0.734473	0.955697	0.300247	0.065*	
H3B	0.741502	0.788389	0.387941	0.065*	
C4	0.8868 (2)	0.8311 (3)	0.5424 (2)	0.0678 (5)	
H4A	0.974476	0.879267	0.461016	0.102*	
H4B	0.902100	0.844121	0.618805	0.102*	
H4C	0.877991	0.730075	0.570107	0.102*	
C5	0.45427 (17)	0.73166 (15)	0.41577 (15)	0.0372 (3)	
H5	0.533031	0.664725	0.413900	0.045*	
C6	0.32540 (17)	0.65778 (15)	0.55378 (15)	0.0377 (3)	
C7	0.35203 (17)	0.69677 (15)	0.64608 (15)	0.0374 (3)	
C8	0.27063 (18)	0.64773 (17)	0.79956 (16)	0.0418 (3)	
C9	0.2384 (3)	0.4599 (2)	1.03001 (19)	0.0738 (6)	
H9A	0.270856	0.365515	1.078206	0.111*	
H9B	0.273764	0.521748	1.061323	0.111*	
H9C	0.126110	0.453518	1.050550	0.111*	
C10	0.21152 (18)	0.54235 (16)	0.58279 (16)	0.0423 (3)	
C11	−0.0089 (2)	0.3797 (2)	0.7483 (2)	0.0690 (5)	
H11A	−0.084012	0.361710	0.835157	0.103*	
H11B	−0.062337	0.398430	0.677267	0.103*	
H11C	0.047778	0.296859	0.763103	0.103*	
C12	0.40315 (17)	0.79230 (15)	0.28093 (14)	0.0367 (3)	
C13	0.4618 (2)	0.7461 (2)	0.18122 (18)	0.0517 (4)	
H13	0.533604	0.677727	0.196652	0.062*	
C14	0.4127 (3)	0.8027 (2)	0.05800 (19)	0.0644 (6)	
H14	0.453637	0.772789	−0.009399	0.077*	
C15	0.3053 (2)	0.9015 (2)	0.03454 (17)	0.0610 (5)	
H15	0.271768	0.937716	−0.047350	0.073*	
C16	0.2476 (2)	0.94653 (18)	0.13404 (16)	0.0484 (4)	
C17	0.29670 (17)	0.89409 (16)	0.25580 (15)	0.0394 (3)	

H17	0.258100	0.927269	0.320979	0.047*	
N1	0.47794 (14)	0.80099 (13)	0.58181 (12)	0.0385 (3)	
N2	0.52250 (15)	0.84889 (13)	0.43155 (12)	0.0392 (3)	
O1	0.58506 (15)	0.78306 (15)	0.75542 (12)	0.0574 (3)	
O2	0.22293 (17)	0.48679 (14)	0.50806 (14)	0.0631 (4)	
O3	0.09960 (14)	0.50348 (13)	0.70232 (13)	0.0560 (3)	
O4	0.18874 (17)	0.72005 (15)	0.83908 (14)	0.0664 (4)	
O5	0.30539 (15)	0.51832 (13)	0.87923 (11)	0.0537 (3)	
Br1A	0.08949 (17)	1.08438 (13)	0.11124 (14)	0.05769 (15)	0.5862
Br1B	0.1173 (3)	1.0792 (3)	0.0900 (3)	0.1081 (10)	0.4138

Atomic displacement parameters (Å²)

	U^{11}	U^{22}	U^{33}	U^{12}	U^{13}	U^{23}
C1	0.0449 (8)	0.0403 (8)	0.0409 (8)	0.0084 (6)	−0.0182 (6)	−0.0210 (6)
C2	0.0429 (8)	0.0422 (8)	0.0438 (8)	0.0011 (6)	−0.0158 (6)	−0.0188 (7)
C3	0.0417 (8)	0.0765 (12)	0.0409 (8)	−0.0126 (8)	−0.0039 (7)	−0.0272 (8)
C4	0.0453 (10)	0.0867 (15)	0.0733 (13)	0.0103 (9)	−0.0232 (9)	−0.0359 (11)
C5	0.0362 (7)	0.0378 (7)	0.0373 (7)	0.0047 (5)	−0.0116 (6)	−0.0168 (6)
C6	0.0399 (7)	0.0346 (7)	0.0349 (7)	0.0042 (6)	−0.0137 (6)	−0.0117 (6)
C7	0.0356 (7)	0.0366 (7)	0.0359 (7)	0.0069 (5)	−0.0108 (6)	−0.0134 (6)
C8	0.0396 (8)	0.0439 (8)	0.0382 (8)	0.0050 (6)	−0.0104 (6)	−0.0167 (7)
C9	0.0947 (16)	0.0698 (13)	0.0363 (9)	0.0047 (11)	−0.0136 (9)	−0.0103 (9)
C10	0.0438 (8)	0.0374 (7)	0.0412 (8)	0.0031 (6)	−0.0168 (7)	−0.0121 (6)
C11	0.0573 (11)	0.0614 (12)	0.0733 (13)	−0.0196 (9)	−0.0058 (10)	−0.0241 (10)
C12	0.0371 (7)	0.0409 (7)	0.0307 (7)	−0.0047 (6)	−0.0057 (6)	−0.0171 (6)
C13	0.0526 (10)	0.0586 (10)	0.0471 (9)	−0.0028 (8)	−0.0030 (7)	−0.0322 (8)
C14	0.0738 (13)	0.0832 (14)	0.0400 (9)	−0.0215 (11)	0.0041 (9)	−0.0400 (10)
C15	0.0740 (13)	0.0699 (12)	0.0313 (8)	−0.0236 (10)	−0.0151 (8)	−0.0154 (8)
C16	0.0523 (9)	0.0460 (8)	0.0394 (8)	−0.0105 (7)	−0.0199 (7)	−0.0095 (7)
C17	0.0414 (8)	0.0450 (8)	0.0320 (7)	−0.0012 (6)	−0.0116 (6)	−0.0173 (6)
N1	0.0387 (6)	0.0437 (7)	0.0328 (6)	0.0016 (5)	−0.0103 (5)	−0.0173 (5)
N2	0.0428 (7)	0.0424 (6)	0.0310 (6)	−0.0011 (5)	−0.0130 (5)	−0.0144 (5)
O1	0.0644 (8)	0.0741 (8)	0.0392 (6)	0.0039 (6)	−0.0209 (5)	−0.0274 (6)
O2	0.0767 (9)	0.0566 (7)	0.0574 (7)	−0.0117 (6)	−0.0126 (6)	−0.0297 (6)
O3	0.0482 (7)	0.0557 (7)	0.0564 (7)	−0.0121 (5)	−0.0033 (6)	−0.0245 (6)
O4	0.0697 (9)	0.0660 (8)	0.0554 (7)	0.0218 (7)	−0.0032 (6)	−0.0297 (7)
O5	0.0660 (8)	0.0486 (6)	0.0363 (6)	0.0124 (5)	−0.0126 (5)	−0.0128 (5)
Br1A	0.0563 (3)	0.0541 (3)	0.0611 (2)	0.0139 (2)	−0.0361 (2)	−0.0164 (2)
Br1B	0.1041 (15)	0.0955 (10)	0.1272 (17)	0.0249 (8)	−0.0824 (13)	−0.0302 (9)

Geometric parameters (Å, º)

C1—O1	1.2062 (18)	C9—H9A	0.9600
C1—N1	1.3765 (19)	C9—H9B	0.9600
C1—C2	1.507 (2)	C9—H9C	0.9600
C2—C4	1.519 (2)	C10—O2	1.202 (2)
C2—C3	1.527 (2)	C10—O3	1.329 (2)

C2—H2	0.9800	C11—O3	1.447 (2)
C3—N2	1.481 (2)	C11—H11A	0.9600
C3—H3A	0.9700	C11—H11B	0.9600
C3—H3B	0.9700	C11—H11C	0.9600
C4—H4A	0.9600	C12—C17	1.381 (2)
C4—H4B	0.9600	C12—C13	1.387 (2)
C4—H4C	0.9600	C13—C14	1.392 (3)
C5—N2	1.4903 (19)	C13—H13	0.9300
C5—C12	1.5110 (19)	C14—C15	1.367 (3)
C5—C6	1.523 (2)	C14—H14	0.9300
C5—H5	0.9800	C15—C16	1.375 (3)
C6—C7	1.338 (2)	C15—H15	0.9300
C6—C10	1.466 (2)	C16—C17	1.380 (2)
C7—N1	1.3801 (19)	C16—Br1B	1.754 (3)
C7—C8	1.507 (2)	C16—Br1A	1.961 (2)
C8—O4	1.190 (2)	C17—H17	0.9300
C8—O5	1.3131 (19)	N1—N2	1.4444 (16)
C9—O5	1.447 (2)		

O1—C1—N1	124.11 (15)	H9A—C9—H9C	109.5
O1—C1—C2	129.17 (14)	H9B—C9—H9C	109.5
N1—C1—C2	106.72 (12)	O2—C10—O3	124.51 (15)
C1—C2—C4	110.91 (14)	O2—C10—C6	122.90 (15)
C1—C2—C3	103.61 (12)	O3—C10—C6	112.54 (14)
C4—C2—C3	114.19 (15)	O3—C11—H11A	109.5
C1—C2—H2	109.3	O3—C11—H11B	109.5
C4—C2—H2	109.3	H11A—C11—H11B	109.5
C3—C2—H2	109.3	O3—C11—H11C	109.5
N2—C3—C2	106.03 (12)	H11A—C11—H11C	109.5
N2—C3—H3A	110.5	H11B—C11—H11C	109.5
C2—C3—H3A	110.5	C17—C12—C13	119.18 (14)
N2—C3—H3B	110.5	C17—C12—C5	120.30 (12)
C2—C3—H3B	110.5	C13—C12—C5	120.52 (15)
H3A—C3—H3B	108.7	C12—C13—C14	119.69 (18)
C2—C4—H4A	109.5	C12—C13—H13	120.2
C2—C4—H4B	109.5	C14—C13—H13	120.2
H4A—C4—H4B	109.5	C15—C14—C13	121.00 (16)
C2—C4—H4C	109.5	C15—C14—H14	119.5
H4A—C4—H4C	109.5	C13—C14—H14	119.5
H4B—C4—H4C	109.5	C14—C15—C16	118.90 (16)
N2—C5—C12	110.97 (11)	C14—C15—H15	120.5
N2—C5—C6	101.25 (11)	C16—C15—H15	120.5
C12—C5—C6	116.58 (12)	C15—C16—C17	121.17 (17)
N2—C5—H5	109.2	C15—C16—Br1B	115.19 (16)
C12—C5—H5	109.2	C17—C16—Br1B	123.57 (16)
C6—C5—H5	109.2	C15—C16—Br1A	121.65 (14)
C7—C6—C10	127.27 (14)	C17—C16—Br1A	117.17 (13)
C7—C6—C5	109.39 (13)	Br1B—C16—Br1A	7.44 (12)

C10—C6—C5	122.35 (13)	C16—C17—C12	120.03 (14)
C6—C7—N1	110.20 (12)	C16—C17—H17	120.0
C6—C7—C8	131.71 (14)	C12—C17—H17	120.0
N1—C7—C8	118.09 (13)	C1—N1—C7	130.55 (13)
O4—C8—O5	126.49 (15)	C1—N1—N2	114.06 (11)
O4—C8—C7	123.05 (14)	C7—N1—N2	109.22 (11)
O5—C8—C7	110.44 (13)	N1—N2—C3	103.78 (11)
O5—C9—H9A	109.5	N1—N2—C5	105.01 (10)
O5—C9—H9B	109.5	C3—N2—C5	116.32 (13)
H9A—C9—H9B	109.5	C10—O3—C11	116.75 (14)
O5—C9—H9C	109.5	C8—O5—C9	116.16 (15)

Hydrogen-bond geometry (Å, º)

D—H···*A*	*D*—H	H···*A*	*D*···*A*	*D*—H···*A*
C9—H9*A*···O1^{i}	0.96	2.42	3.258 (3)	146
C14—H14···O1^{ii}	0.93	2.53	3.418 (2)	161
C11—H11*B*···O2^{iii}	0.96	2.60	3.533 (3)	164
C3—H3*B*···O2^{iv}	0.97	2.62	3.514 (3)	154

Symmetry codes: (i) −*x*+1, −*y*+1, −*z*+2; (ii) *x*, *y*, *z*−1; (iii) −*x*, −*y*+1, −*z*+1; (iv) −*x*+1, −*y*+1, −*z*+1.

Comparison of the selected experimental and calculated geometric parameters (Å, °)

Bond lengths	***X-ray***	***DFT***
O1—C1	1.206 (2)	1.209
C1—N1	1.377 (2)	1.384
N1—N2	1.444 (2)	1.438
N1—C7	1.380 (2)	1.374
C3—N2	1.481 (2)	1.470
C5—N2	1.490 (2)	1.484
C8—O4	1.190 (2)	1.199
C8—O5	1.313 (2)	1.334
C10—O2	1.202 (2)	1.212
C10—O3	1.329 (2)	1.351
O3—C11	1.447 (2)	1.438
O5—C9	1.447 (2)	1.443
C16—Br1A/Br1B	1.961 (2)/1.754 (3)	1.922
Angles		
O1—C1—N1	124.1 (2)	125.7
O1—C1—C2	129.2 (2)	129.2
N1—C1—C2	106.7 (2)	105.1
C1—N1—C7	130.6 (2)	133.8
C1—N1—N2	114.1 (2)	113.1
C3—N2—C5	116.3 (2)	119.8
C7—C8—O4	123.1 (2)	122.9
C7—C8—O5	110.4 (2)	110.8
O4—C8—O5	126.5 (2)	126.3

C6—C10—O2	122.9 (2)	123.9
C6—C10—O3	112.5 (2)	112.4
O2—C10—O3	124.5 (2)	123.6
C10—O3—C11	116.8 (2)	115.7
C8—O5—C9	116.2 (2)	115.2
C15—C16—Br1A/Br1B	121.7 (2)/115.2 (2)	119.2
C17—C16—Br1A/Br1B	117.2 (2)/123.6 (2)	119.1

Quantum chemical parameters of the title compound calculated by B3LYP/6-311G (d, p)

E_T(eV)	101131.745
E_{HOMO} (eV)	–6.026
E_{LUMO} (eV)	–1.868
$DE_{(LUMO–HOMO)}$ (eV)	4.158
Chemical hardness (η)	2.079
Chemical Softness (ξ)	0.241
Chemical potential (μ)	3.947
Electrophilicity (ψ)	3.754
Electronegativity (χ)	–3.947
Dipole moment (D)	3.847

$\eta = 1/2[E_{LUMO}-E_{HOMO}]$, $\xi = 1/2\eta$, $\mu = [1/2(E_{LUMO}+E_{HOMO})]$, $\psi = \mu^2/2\eta$, $\chi = -\mu$